Materials Science and Engineering B 174 (2010) 55–58

Contents lists available at ScienceDirect

Materials Science and Engineering B

journal homepage: www.elsevier.com/locate/mseb

Effect of Pb-doping on the morphology, structural and optical properties of ZnO nanowires synthesized via modified thermal evaporation

Mashkoor Ahmad, Caofeng Pan, Wang Yan, Jing Zhu*

Beijing National Center for Electron Microscopy, The State Key Laboratory of New Ceramics and Fine Processing, Department of Material Science and Engineering, Tsinghua University, Beijing 100084, China

ARTICLE INFO

Article history:
Received 25 August 2009
Received in revised form 16 March 2010
Accepted 16 March 2010

Keywords:
ZnO
Pb-doped
Crystalline
Photoluminescence

ABSTRACT

Pb-doped ZnO nanowires (NWs) have been synthesized by modified thermal evaporation method. Effect of Pb-doping on the morphology, structure, and optical properties of as deposited NWs have been investigated. The TEM images show that the doped NWs consist of cantilever-like with diameter in the range of 20–150 nm. It has been found that the doped NWs are single crystalline grown along [1 0 1] direction. The composition and valence state of Pb ions have been investigated through energy dispersive spectroscopy (EDS) and X-ray photospectroscopy (XPS), which demonstrate that the Pb ions are uniformly doped into each NW and are in +2 oxidation state. In addition, photoluminescence spectra exhibit an increased amount of defects with increasing Pb, which leads to a red shift in the UV region. Furthermore, the band gap tailoring in Pb-doped ZnO NWs makes their potential for optoelectronics devices.

1. Introduction

ZnO is one of the most promising materials because of a direct wide band gap $E_g = 3.37$ eV and large exciting binding energy 60 meV at room temperature. It has been found useful in many applications such as optoelectronic devices, surface acoustic wave devices, field emitters, piezoelectric, transparent conducting materials and solar cells [1–7]. Recently, intensive research has been focused on fabricating one-dimensional (1D) ZnO nanostructures such as nanotubes, nanowires (rods), and nanobelts (rings) due to their shape induced novel properties and potential applications [8–10]. The synthetic methods reported of 1D ZnO nanowires and nanorods include chemical vapor deposition [11], low-temperature wet-chemical methods [12], thermal evaporation [13], and hydrothermal syntheses [14,15].

On the other hand, doping of semiconductor with selective elements [16,17] offers an effective approach to adjust the electrical, optical and magnetic properties, which is crucial for their practical applications. Although a mass of research has been done on nanostructure doping, it still remains a challenge to achieve high quality crystalline with excellent optical and electrical properties in doped one-dimensional ZnO nanostructures. Furthermore, although some groups already focused their work on Pb-doping in ZnO [18,19], however, the detailed study of Pb-doping is still required to understand the role of Pb in ZnO NWs. As the ionic radius of Pb^{2+} (1.19 Å) is larger than Zn^{2+} (0.74 Å), Zn is more active in chemical reaction then Pb. In vapor reaction Pb can be easily substituted by Zn and become Pb-doped ZnO nanomaterial. The main focus of the present work is to investigate the effect of Pb-doping in ZnO NWs for the future optoelectronics applications.

2. Experimental

Synthesis of un-doped and Pb-doped ZnO NWs were carried out in a horizontal quartz tube furnace via thermal evaporation method, where the temperature, pressure and flow rates of working gases are well controlled. In this process, a crucible containing the mixture of metallic Zn powder (3 g) and Pb_2O_3 (99.998%, Aldrich) powders (0, 0.5, 1, 2 g) were respectively added, placed in the central region of the quartz tube furnace and heated to 550 °C for 3 h. Ar carrier gas with an O_2 content of 5% flows through the quartz tube at a rate of 150 standard cubic centimeter/min (sccm). A Si substrate cleaned carefully, followed by supersonically in acetone, alcohol and de-ionized water for 30 min and mounted downward region of the furnace where the temperature was 450 °C. Two samples were prepared in our experiments, i.e. ZnO nanowires with or without Pb-doping. After the reaction completed, the as-prepared products were examined by X-ray diffraction (XRD) with Cu Kα radiation, $\lambda = 1.5418$ Å, scanning electron microscope (SEM-6301F operated at 15 kV), high resolution transmission electron microscope (HRTEM-JEM2011 operated at 200 kV), energy dispersive spectroscopy (EDS) and X-ray photospectroscopy (XPS). PL measurement was conducted at room temperature using the 325 nm line of a He–Cd laser as the excitation source.

---

* Corresponding author. Fax: +86 10 62771160.
E-mail address: jzhu@mail.tsinghua.edu.cn (J. Zhu).

0921-5107/$ – see front matter © 2010 Elsevier B.V. All rights reserved.
doi:10.1016/j.mseb.2010.03.039

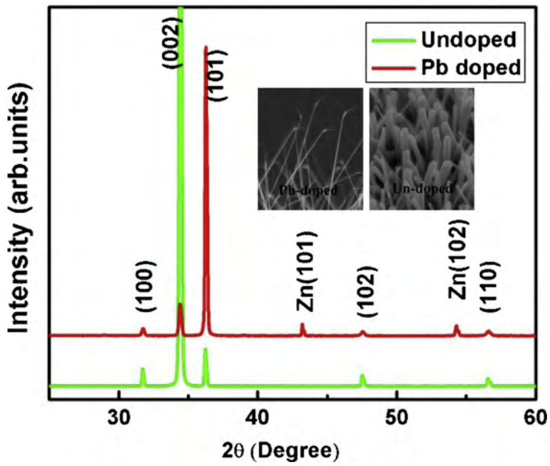

Fig. 1. XRD pattern of un-doped and Pb-doped with (3:1) ratio ZnO nanowires. The inset shows the SEM images of the both products.

3. Results and discussions

The crystal structure and phase purity of as deposited products has been characterized using XRD. Fig. 1 shows the XRD patterns of the Pb-doped and un-doped ZnO nanowires (NWs) grown on Si substrate. All the major diffraction peaks in the pattern can be index to pure ZnO wurtzite crystal structure. The presence of two weak Zn peaks in the pattern reveals that a small amount of Zn powder remains phase separated during the experiment. It is also found that the intensity of (1 0 1) peak is much stronger than that of other peaks. The high intensity of (1 0 1) peak shows that the doped nanowires are preferably grown along the [1 0 1] direction. The doped Pb does not alter the crystal structure but it causes the slight shift in all peaks. The evaluated *c*-axis lattice constant of the Pb-doped NWs is 0.5240 nm, which is much larger than that of un-doped ZnO ($c = 0.5109$ nm) NWs. The change in the lattice constants confirms the successful substitution of Pb atoms into ZnO lattice. The increase in the lattice of doped NWs can be understood as the ionic radius of Pb^{2+} (1.19 Å), dopant is larger than that of Zn^{2+} (0.74 Å). Furthermore, there are also some changes in the intensity of diffraction peaks as compare to un-doped NWs, which may be attributed to the crystalline quality of the NWs.

Field emission scanning electron microscopy has been employed to analyze the microstructural characteristics of the as-grown products. Fig. 2(a) shows the morphology of as-grown un-doped and Pb-doped NWs. The morphology of un-doped sample shows that the product consists of oriented straight NWs with uniform diameter in the range of ~50–300 nm and length in the range of microns as shown in Fig. 2(a) inset. However, the morphology of doped sample reveals the cantilever-like NWs with a little amount of particles as shown in Fig. 2(b). The diameter of doped NWs in the bottom region is uniform and in the range of ~20–150 nm. Most of the NWs have length in the range of hundred of microns. These results clearly indicate the effect of Pb-doping on the morphology of ZnO NWs.

In order to further investigate the microstructure of prepared samples, the HRTEM and SAED measurements have been carried out over individual un-doped and Pb-doped NWs, as shown in Fig. 3(a–c). It is observed that the un-doped NW has a wurtzite structure and the growth direction is oriented along [0 0 1] as shown in Fig. 3(a). The HRTEM image and corresponding SAED over a dozen of Pb-doped NWs is performed as shown in Fig. 3(b). From HRTEM images it is found that the surfaces of Pb-doped NWs have ripple-like edges which may appear due to the Pb incorporation. The interplanar distance of fringes is measured to be 0.24 nm, which correspond to the spacing of (1 0 1) planes of wurtzite ZnO. The corresponding SAED pattern for each NW is found to be identical to the entire part of Pb-doped ZnO NW as shown in Fig. 3(b) inset. The doped NWs are found to be single crystalline grown along [1 0 1] direction. These results are also consistent with the XRD measurement, in which intensity of (1 0 1) diffraction peak is higher than that of other peaks, suggesting that (1 0 1) crystal face should be the primary face of the Pb-doped NWs. The surface of NWs looks to be a little rough due to the influence of Pb particles as shown in Fig. 3(c).

The amount of Pb-doping has been investigated through EDS elemental analysis. Fig. 3(d) shows the EDS for single Pb-doped NW from the area indicated by arrow in the TEM image (inset). An oxygen peak at about 0.52 keV and Zn peaks at about 1.02, 8.67 and 9.60 keV can be observed in the spectra. The signals of Cu, C and Cr peaks come from the surface of copper grid used for TEM measurement. The Pb peaks also appear at about 2.34 keV as reported [18]. Quantitative analysis reveals that the average amount of Pb contents is about 2% in each Pb-doped ZnO NW. Statistical analysis of EDS measurements over dozen of Pb-doped NWs demonstrates that the variation of Pb content is rather small and the composition of Pb dopant is uniform throughout the specimen. Therefore EDS results further demonstrate that Pb is incorporated into ZnO, which is also in good agreement with the XRD results.

The valence state of the Pb element has been analyzed by XPS. Fig. 4(a) shows the XPS survey of the Pb-doped sample. The Pb-doped sample shows that the Pb peaks are located at 139.2 and 143.8 eV corresponding to the electronic states of $Pb4f_{7/2}$ and $Pb4f_{5/2}$, respectively, as shown in Fig. 3(b). The existence of small satellite peaks in the spectrum show that Pb is in +2 oxidation state and successfully substituted into lattice. From the peak position it is observed that the Pb binding energy peaks are slightly shifted

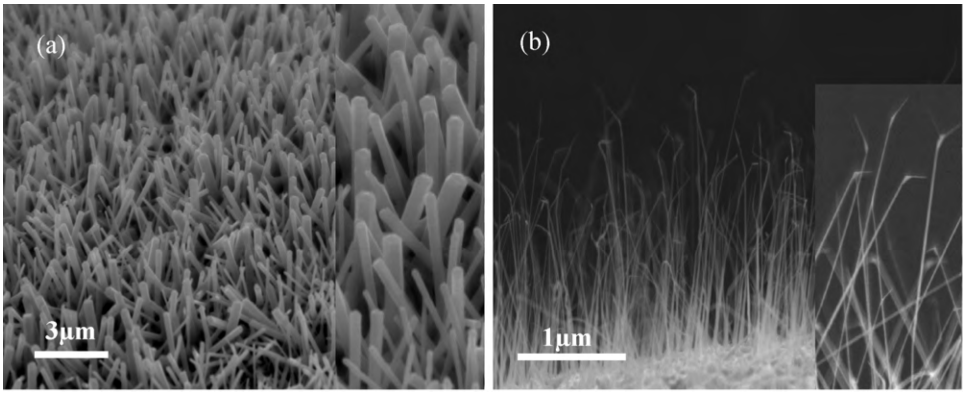

Fig. 2. Field emission scanning electron microscopy images: (a) un-doped ZnO nanowires; (b) Pb-doped NWs with (3:1) ratio.

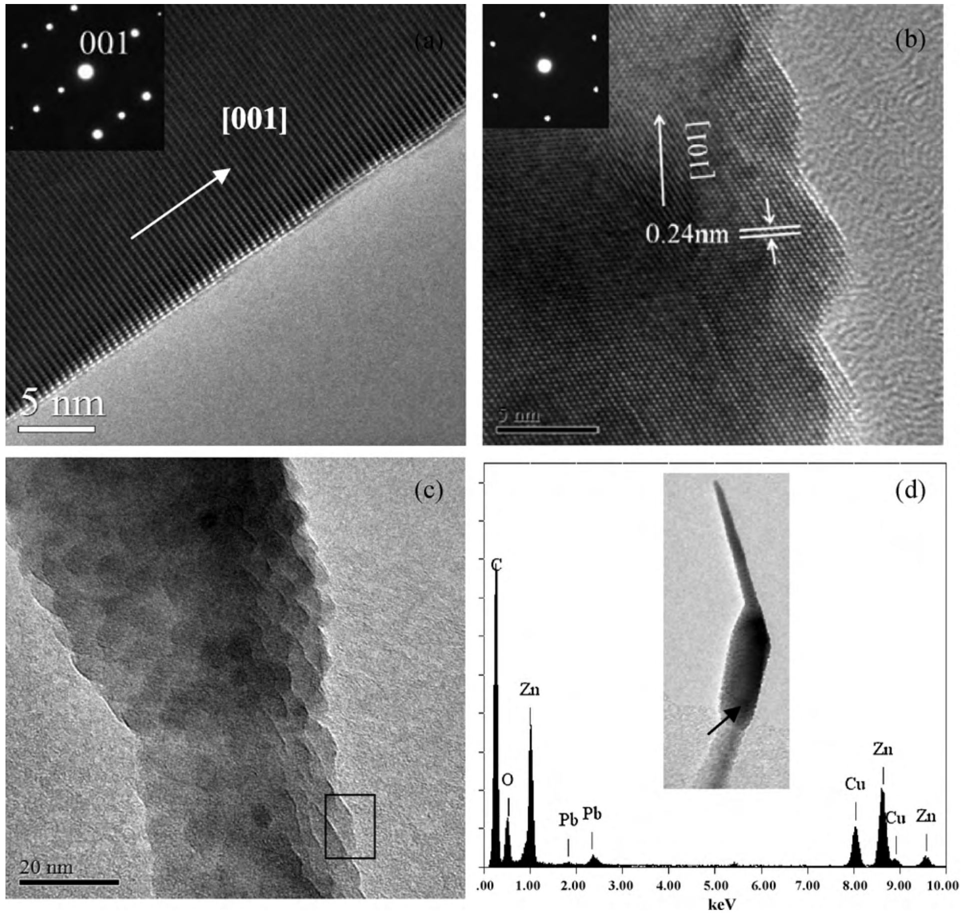

Fig. 3. HRTEM images and their corresponding SAED patterns (inset): of (a) un-doped nanowire along [0 0 1] growth direction (b) Pb-doped (3:1) ZnO grown along [1 0 1] direction. (d) TEM image of doped nanowires. (c) EDS spectra of Pb-doped ZnO nanowires. Inset is a display of individual TEM image of Pb-doped ZnO nanowire.

towards lower binding energy side with respect to the reported [20] and have the same energy difference about 4.6 eV. The shift in binding energy peaks is due to the successful incorporation of Pb into ZnO NWs. Furthermore, the average contents of Pb are also consistent with EDS measurements (Fig. 3d).

The doping in ZnO has great influence on tuning the optical and electrical properties of NWs. Fig. 5 shows the room temperature PL spectra of un-doped and Pb-doped NWs with ratios (3:0, 3:0.5, 3:1, 3:2). The un-doped NWs consist of a strong UV band peak at 378 nm and a weak broad green band centered at about 530 nm. As compared with un-doped NWs, the doped NWs exhibit three major changes in the spectrum which makes it interesting for the discussion. Firstly, a large red shift of about 10 nm in UV emission, secondly, the increase of green emission band (which usually corresponds to deep-level defect transitions) and thirdly the decrease in the intensity of UV emission. The red shift in UV (inset Fig. 5), in other words, the narrowing in the band gap with increase in Pb-doping may be due to the strong sp–d exchange interactions between the band electrons of ZnO and the localized “d” electrons of Pb^{2+} ions, which form band impurity states near the bottom of the conduction band [21]. The merging of these impurity states with the bottom of the conduction band may give rise to the narrowing of the band gap. The shrinkage of the band gap towards the visible range is normally induced by the introduction of impu-

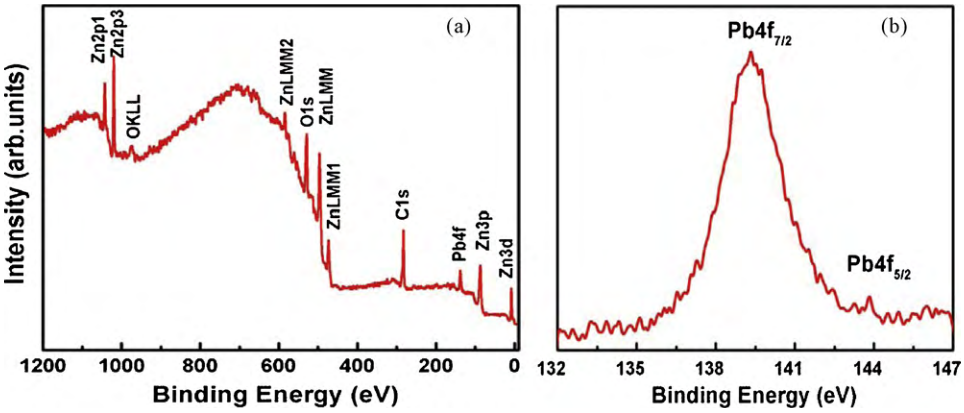

Fig. 4. XPS spectra of Pb-doped (3:1) ZnO nanowires: (a) complete survey, (b) Pb4f.

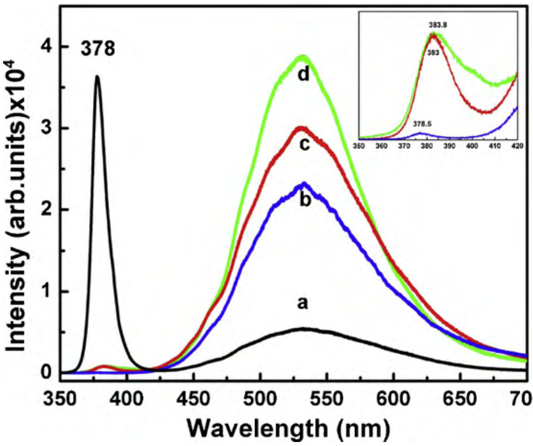

Fig. 5. Room temperature PL spectra of un-doped and Pb-doped ZnO nanowires with ratios [a = 3:0, b = 3:0.5, c = 3:1, d = 3:2].

rity into the semiconductor [22–25]. The origin of green emission band in the ZnO band gap has been studied intensively and is considered to be due to the singly ionized oxygen vacancies, which are responsible for this emission results from the recombination of a photogenerated hole with a singly ionized charge state [26]. Lastly, the decrease in the intensity of UV emission and increase in green emission intensity indicates that the amount of defects (like Zn interstitials) may increase with the increase in Pb-doping [27], which suppresses the excitonic emission of the doped NWs.

4. Conclusions

In conclusion, Pb-doped ZnO NWs have been successfully synthesized via a thermal evaporation method. It has been found that Pb dopant has strong influence on the morphology, structure and the photoluminescence properties of the ZnO NWs. The morphology of doped NWs is found to be cantilever-like nanostructure. Furthermore, the Pb-doped NWs are found to be a single crystalline along [1 0 1] growth direction. In addition, photoluminescence spectroscopy exhibits a red shift in the near band edge (NBE) due to the merging of impurity levels with edge of conduction band. The tailoring in band gap of doped nanowires makes their potential for the fabrication of novel nanoscale devices. These NWs could be useful in the fabrication of future optoelectronic nanodevices such as nanosensors, scanning nanoprobes and field emission, etc.

Acknowledgment

This work is financially supported by National 973 Project of China and Chinese National Nature Science Foundation. The authors are also grateful to the Higher Education Commission (HEC) and PINSTECH (PAEC) Pakistan for the financial support to Mashkoor Ahmad.

References

[1] M.H. Huang, S. Mao, H. Feick, H.Q. Yan, Y.Y. Wu, H. Kind, E. Weber, R. Russo, P.D. Yang, Science 292 (2001) 1897.
[2] T. Aoki, Y. Hatanaka, D.C. Look, Appl. Phys. Lett. 76 (2000) 3257.
[3] A. Bousfia, E.H. El Boudouti, D. Bria, A. Nougaoui, B. Djafan-Rouhani, V.R. Velasco, J. Appl. Phys. 87 (2000) 4507.
[4] C.J. Lee, T.J. Lee, S.C. Lyu, Y. Zhang, H. Ruh, H.J. Lee, Appl. Phys. Lett. 81 (2002) 3648.
[5] G. Sberveglieri, S. Groppelli, P. Nelli, A. Tintinelli, G. Giunta, Sens. Actuators B 25 (1995) 588.
[6] D.S. Ginley, C. Bright, Mater. Res. Soc. Bull. 25 (2000) 15.
[7] W.E. Devaney, W.S. Chen, J.M. Stewart, R.A. Mickelsen, IEEE Trans. Electron. Devices 37 (1990) 428.
[8] Z. Pan, Z. Dai, Z.L. Wang, Science 291 (2001) 1947.
[9] X. Kong, Y. Ding, R. Yang, Z.L. Wang, Science 303 (2004) 1348.
[10] C.H. Liu, J.A. Zapien, Y. Yao, X.M. Meng, C.S. Lee, S.S. Fan, Y. Lifshitz, S.T. Lee, Adv. Mater. 15 (2003) 838.
[11] G.Z. Wang, N.G. Ma, C.J. Deng, P. Yu, C.Y. To, N.C. Hung, M. Aravind, H.L. Ng Dickon, Mater. Lett. 58 (2004) 2195.
[12] J.H. Choy, E.S. Jang, J.H. Won, J.H. Chung, D.J. Jang, Y.W. Kim, Adv. Mater. 15 (2003) 1911.
[13] V.A. Roy, A.B. Djurisic, W.K. Chan, J. Gao, H.F. Lui, C. Surya, Appl. Phys. Lett. 83 (2003) 141.
[14] L. Vayssieres, Adv. Mater. 15 (2003) 464.
[15] B. Liu, C. Zeng, J. Am. Chem. Soc. 125 (2003) 4430.
[16] J.H. He, C.S. Lao, L.J. Chen, D. Davidovic, Z.L. Wang, J. Am. Chem. Soc. 127 (2005) 16376.
[17] M. Ahmad, J. Zhao, J. Iqbal, W. Miao, L. Xie, R. Mo, J. Zhu. J. Phys. D Appl. Phys. 42 (2009) 165406.
[18] M.Z. Shao, H.Z. Xiao, M.M. Xiang, K.W. Shi, T.L. Shuit, Phys. Stat. Sol. (a) 202 (2005) 405.
[19] D. Chu, Y.P. Zeng, D. Jiang, Mater. Lett. 60 (2006) 2783.
[20] T. Yoshida, T. Yamaguchi, Y. Iida, S. Nakayama, J. Nucl. Sci. Technol. 40 (2003) 672.
[21] K. Vanheusden, W.L. Warren, J.A. Voigt, C.H. Seager, D.R. Tallant, Appl. Phys. Lett. 67 (1995) 1280.
[22] J. Jie, G. Wang, X. Han, Q. Yu, Y. Liao, G. Li, J. Hou, Chem. Phys. Lett. 387 (2004) 466.
[23] S.M. Zhou, X.H. Zhang, X. Meng, K. Zou, X. Fan, S. Wu, S.T. Lee, Nanotechnology 15 (2004) 1152.
[24] P. Yang, H. Yan, S. Mao, R. Russo, J. Johnson, R. Saykally, N. Morris, J. Phan, R. He, H. Choi, Adv. Funct. Mater. 12 (2002) 323.
[25] M. Ahmad, C. Pan, J. Iqbal, L. Gan, J. Zhu, Chem. Phys. Lett. 480 (2009) 105.
[26] T. Massalski, Binary Alloy Phase Diagrams, ASM International, Metals Park, OH, 1993, p. 184.
[27] N.F. Mott, Metal–Insulator Transitions, Taylor and Francis, London, 1974.